Surface & Coatings Technology 362 (2019) 282–292

Contents lists available at ScienceDirect

Surface & Coatings Technology

journal homepage: www.elsevier.com/locate/surfcoat

Role of micro-dimple array geometry on the biological and tribological performance of Ti6Al4V for biomedical applications

M. Sadeghi, M. Kharaziha*, H.R. Salimijazi, E. Tabesh

Department of Materials Engineering, Isfahan University of Technology, Isfahan 84156-83111, Iran

ARTICLE INFO

Keywords:
Micro-dimple array
Laser surface texturing
Friction coefficient
Wear mechanism

ABSTRACT

The purpose of this study was to employ surface texturing, using CO_2 pulsing laser, to create micro-dimple arrays and study the role of diverse geometries of micro-dimples on the physical, biological and tribological responses of Ti6Al4V. Scanning electron microscopy and X-ray diffraction were applied to study the structural and chemical composition of surface treated samples, respectively. Furthermore, the effects of laser treatment on the surface hydrophilicity, topography and hardness of samples were investigated using water contact angle measurement, surface roughness tester and micro-hardness tester. Results confirmed the noticeable role of scan rate (0.5, 1, 5 and 10 mm/s) on the morphology of micro-dimples, the chemical structure and hardness of the samples. In this respect, increasing the scan rate of laser irradiation from 0.5 mm/s to 10 mm/s resulted in the formation of acicular α-Ti around micro-dimples with various thicknesses. Moreover, micro-hardness of Ti6Al4V greatly improved to 635 ± 21 HV, when the scan rate enhanced to 5 mm/s. In addition, the effect of surface texturing on the attachment, proliferation and spreading of MG63 cells were investigated. Results confirmed that cell proliferation was significantly improved on the textured Ti6Al4V. Tribological characterization revealed that poor tribological properties of TiO_2 layers on Ti6Al4V could be meaningfully modified using laser texturing, depending on the geometries of micro-dimples. Additionally, noticeably reduction of friction was obtained on the textured samples. In summary, laser texturing could be effectively applied to simultaneously enhance the tribological and biological performances of Ti6Al4V alloy for biomedical applications.

1. Introduction

One of the important present challenges in orthopedic is the total joint replacements, particularly hip and knee, and a rising tendency to substitute damaged tissue with artificial organs [1]. Total joint replacements are commonly fabricated from a metal femoral component which articulates with a polyethylene tibial. Every year, there is a large number of replacing joint implant surgery, due to failure or destruction caused by mechanical loosening and instability, often leading to osteolysis [2]. Therefore, improvement of wear behavior of knee replacement components is the main challenge. Among various biomedical metals, titanium and cobalt-based alloys are the most common groups of biomaterials applied for knee replacements [1]. Thanks to their good biocompatibility and corrosion resistance, and high strength to weight ratio, titanium and its alloys are extensively applied in orthopedic and dental implants [3]. Titanium is an allotropic metal that has a hexagonal closed packed (HCP) crystalline structure at temperatures below 885 °C (α), and a body-centered cubic (BCC) structure at temperatures above 885 °C (β). Ti6Al4V, which is the main titanium alloy for biomedical applications, is an alpha + beta (α + β) alloy reveling excellent ductility and strength after heat-treatment processes [4,5]. Despite the fantastic properties of Ti6Al4V, due to low work hardening, weak shear strength and inability to protect the substrate from wear, and high friction coefficient, the biomedical applications of this alloy are limited [6].

Recently, a variety of surface treatment and coating approaches have been employed to improve wear behavior of titanium and its alloys [7]. Surface engineering is stated as any process directing to promote the functionality of material surface by adjusting its geometric state (such as roughness, shape and, texture), chemical composition and microstructure. Between these approaches, the tribological properties of Ti alloys could be effectively improved via surface hardening [8], surface coating [9], thermal oxidation [10], anodization [11] and laser engineering [12]. In addition, previous studies confirmed that biocompatibility of titanium alloys is strictly depended on the surface topography, composition, and roughness of titanium alloys [13]. For instance, Grizon et al. [14] suggested that titanium with rough surfaces provided greater bone response than smooth surfaces. Between

* Corresponding author.
E-mail address: kharaziha@cc.iut.ac.ir (M. Kharaziha).

https://doi.org/10.1016/j.surfcoat.2019.01.113
Received 7 September 2018; Received in revised form 13 January 2019; Accepted 31 January 2019
Available online 01 February 2019
0257-8972/

different methods, surface engineering by using laser is a promising strategy in which melt and/or heat were applied to texture or alter the surface of substrates [15]. Between various biomedical applications of the laser, surface melting is a promising technique to enhance the hardness and corrosion resistance of Ti6Al4V alloy [16]. Moreover, laser surface texturing is an environmentally friendly method with a controllable order which could modulate the surface topography and increase the surface energy, wettability, protein and cell adhesion compared to the commercially available alloys [12]. Previous results confirmed that, compared to smooth bearing surfaces, micro-textured substrates could promote load-carrying capacity and diminish friction and wear [17]. Chen et al. [18] reported that micro-textures like micro-grooves developed using Nd: YAG laser improved cell and protein adhesion on Ti6Al4V surfaces. In another study, Yue et al. [19] developed circular, square and elliptical shapes of textures with almost the same area density using CO_2 laser and reported the influence of textured surface on the reduction of the coefficient friction of Ti6Al4V alloy. Kumari et al. [20] developed surface textured Ti6Al4V with liner and dimple geometries, using ArF excimer laser, and found its improved mechanical properties, cell function and corrosion resistance. Moreover, laser texturing resulted in a reduction in the friction at a load of 5 N. Hue et al. [21] studied the effect of micro-dimples with different densities on the friction behavior of Ti6Al4V. They found that the surface with a higher density of textures had lower friction under dry sliding. Despite the extensive investigates on the surface texturing of titanium alloys using laser techniques, limited studies were focused on the surface texturing by means of CO_2 laser. Moreover, the effects of various laser parameters (such as scan rate of laser process) on the both simultaneously biological and tribological characteristics of the titanium alloys have not been studied.

In this research, we applied pulsing laser beam in the CO_2 atmosphere to develop micro-dimple texture on the surface of Ti6Al4V and studied the function of laser scan rate on their physical, biological and tribological properties. We hypothesized that a micro-textured Ti6Al4V optimized for a prosthetic knee bearing could decrease friction and wear via improvement of lubrication and trapping wear debries in the micro-dimples.

2. Materials and methods

2.1. Materials

Ti6Al4V (chemical composition in wt%: Ti-5.81% Al-4.53% V) was purchased from Sigma with an average hardness of 350 ± 7.6 Hv and an average thickness of 5 mm. Zirconia ball (ZrO_2) was produced by Villeroy & Boch, com, with a surface hardness of 1340 H_V and surface roughness of Ra = 0.05 μm for tribological evolution. For cell culture study, Dulbecco's Modified Eagle Medium (DMEM-low glucose), streptomycin/ penicillin and fetal bovine serum (FBS) were got from Bioidea, Iran. Dimethyl sulfoxide (DMSO) and glutaraldehyde (25%) were purchased from Sigma. MG63 osteoblast-like cell-line was purchased from the National Cell Bank of Iran at the Pasteur Institute (NCBI code: C555).

2.2. Laser texturing process of Ti6Al4V

Laser texturing process was applied by using a CO_2 pulsing laser at a wavelength of 6100 nm and power of 70 W to achieve micro-patterns with dimple geometry. The geometries of micro-dimples were selected based on the previous researches focused on the biomedical applications [22–24]. The input information of CO_2 laser system is presented in Table 1. Supplementary Fig. S1 shows the CO_2 laser system applied for laser treatment approach. Various scan rates of laser process were selected to develop micro-dimple textures with different area densities and diameters, designed by 2D Auto desk AutoCAD software. The designs executed on square-shaped samples are presented in Table 2.

Table 1
CO_2 laser system specifications used in this work.

Laser processing parameters and conditions	
Output wavelength (nm)	6100
Average laser beam power (w)	70
Repetition rate (f)	60 Hz
Scanning speed (v)	0.5–10 mm/s
Operation mode	Pulsed
Number of laser pulses (N)	3
Active medium	CO_2

Ti6Al4V specimens were cut to the square samples with the dimension of 10 mm × 10 mm × 5 mm and discs with a diameter of 50 ± 0.2 mm and thickness of 5 mm, for wear testing (ball on disc). The substrates were polished to get a surface roughness (Ra) of 0.2 μm, before laser process.

2.3. Characterization of laser-textured Ti6Al4V

The microstructure of the laser-textured Ti6Al4V was evaluated by optical and scanning electron microscopy (SEM, Philips, XL30). The diameter of the micro-dimples was determined using ImajeJ software. The phase composition of the samples, before and after laser texturing and wear test, was investigated using X-ray diffraction (XRD, X0 Pert Pro X-ray diffractometer, Phillips, Netherlands, CuKα radiation) ($\lambda = 0.154$ nm).

The profile of micro-hardness of the treated samples was evaluated at 10 points for each sample by using a load of 100 N and 30 s. To determine the depth of micro-dimples, surface roughness tester "SJ-210/310/410" was used. After cleaning the samples by acetone and water, the contact angle of samples was estimated to determine their wettability. In this test, deionized water drops in a volume 0.2 μl were used. The drop image was stored by a Canon camera with a macro-lens and contact angle was measured by Image Analysis Program (Image J) at 5 points in each sample.

2.4. Wear evaluation of laser-textured Ti6Al4V

Tribological properties of the untreated and laser-treated samples were investigated using a pin on disc tribometer (ball on disc configuration) at room temperature and constant humidity. Wear test was carried out by sliding a zirconia ball with 10 mm in diameter, at a constant speed of 0.1 m/s with an applied load of 4.3–12 N/mm for a total distance of 200 m. The selection of alumina ball as the counter-body component was based on its great hardness, wear resistance, chemical inertness and electrical insulating characteristics. Moreover, the experimental wear parameters were selected according to previous researches [22]. The applied load cell range was related to the hip joint loading [25]. The wear behavior of samples was determined by measuring the weight loss (mg) (weight difference at each stage with the initial weight of the disc) of the samples by means of precision balance 0.001 g. Moreover, SEM and XRD techniques were applied to analyze the wear debris, worn surface and explain the wear mechanisms.

2.5. Cell culture

In order to evaluate the effect of laser texturing on the biological behavior of Ti6Al4V, MG63 cell line was cultured on the samples. Before cell seeding, MG63 cells were cultured in DMEM-low glucose supplemented with 10 vol% FBS and 1 vol% streptomycin/penicillin at 37 °C in 5% CO_2. Before cell culture, the samples were sterilized in 70 vol% ethanol for 30 min and then, were exposed to ultraviolet (UV) light for 2 h. Subsequently, the samples were immersed in the complete culture medium, 24 h prior to the cell seeding. The cells with a density of 10^4 cells/well were seeded on the samples and tissue culture plate

Table 2
The properties of micro-textured Ti6Al4V developed using various laser parameters.

Sample	Laser scan speed (mm/s)	Dimple area ratio (%)	Distance of dimples (μm)	Dimples diameter (μm)	Contact angle (°)
Untreated Ti6Al4V (N)		–	–	–	49 ± 4°
L1	10	6.5	600	194 ± 19	37 ± 7
L2	1	13.2	520	260 ± 17	52 ± 3
L3	5	21.2	220	186 ± 5	33 ± 5
L4	0.5	42.6	120	267 ± 10	41 ± 3

(TCP, control) and were incubated for 5 days at 37 °C in 5% CO_2.

2.5.1. Cell proliferation evaluation

The viability of MG63 cells seeded on the samples was examined by 3-(4,5-dimethylthiazolyl-2)-2,5-diphenyl tetrazolium bromide (MTT) assay. At the mentioned culture times, MTT solution with concentration of 0.5 mg/ml in PBS was added to the samples and control ($n = 3$). After incubation for 4 h, the formazan crystals were dissolved using DMSO and the optical density (OD) of the solutions was estimated using a microplate reader (BioTek, 490 nm). Finally, the relative viability of cells (compared to control) was calculated as below [26]:

$$\textit{Relative cell viability } (\%control) = \frac{A_{sample} - A_b}{A_c - A_b} \times 100$$

in which A_{sample}, A_b and A_c are related to the absorbance of the samples, blank (DMSO) and control (TCP), respectively.

2.5.2. Cell morphology study

Attachment and spreading of MG63 cells cultured on the samples for 3 days were evaluated using SEM imaging. After 3 h-fixation of cell-seeded samples using with glutaraldehyde solution (2.5%) and 40-min with 0.1% osmium tetroxide, they were washed with PBS. Consequently, the cell-seeded samples were dehydrated through ethanol series (50%, 70%, 90%, and 100%, each for 20 min), and air dried. After gold coating process, the cell-seeded samples were evaluated using SEM imaging.

2.6. Statistical analysis

The biological data was considered using one-way ANOVA analyses and reported as the mean ± standard deviation (SD). To determine a statistical significant difference between groups, Tukey's *post-hoc* test using GraphPad Prism Software (V.6) with a p-value < 0.05 was applied to be significant.

3. Results and discussion

3.1. Characterization of the laser-textured Ti6Al4V alloy

In order to show the role of micro-texturing on the microstructure, hardness, wettability, biocompatibility and wear behavior of Ti6Al4V, laser process with different scan speeds of laser irradiation was performed leading to the formation of micro-dimples with four different densities and dimple diameters. SEM images of various micro-textured substrates are presented in Fig. 1. Results revealed the formation of defect-free micro-dimples with uniform dimensions, depending on the scan rate of laser irradiation. According to the SEM images, the area density and average diameter of dimples in various samples, as well as the distance between the dimple redial, were calculated and presented in Table 2. According to the applied inputs, the diameters and density of dimples almost enhanced with a reduction in the beam scan rate. Moreover, the distance between dimples decreased with reduction in the scan rate. In addition to dimple's diameter and areal density, the depth of dimples modulated with changing the scan speed of the beam. Fig. 2 shows the difference in the depth of micro-dimples in four different samples (L1, L2, L3, L4), estimated using a roughness meter. Generally, it could be concluded that laser parameters, specifically residence time or scan speed of beam as well as beam diameter affected surface roughness. Results confirmed that the depth of melted zone was in the range of 3–6 μm, depending on the scan speed. While the average depth of dimples in L1 sample (scan rate of beam = 10 mm/s) was about 3 ± 0.3 μm, it was significantly enhanced to about 6.2 ± 0.3 μm at L4 sample (beam scan rate = 0.5 mm/s). Moreover, the enhanced height of the surface at the edge of dimples, due to the formation of piled up material, could be detected at both L2 and L4 samples, while could not be clearly detected at two other samples (Fig. 2a). According to Fig. 2b, when laser beam impacts the surface of the alloy (Fig. 2b(i)), the surface region around the laser point rapidly reached the melting point leading to melting at the center of laser affected zone. This process led to formation of a temperature gradient from the center to the edge of dimples during the laser process. Increasing the laser time resulted in the movement of the interface of liquid/solid phases via diffusion of elements in the liquid phase and, finally, the piled-up of materials at the edge of the molten pool (Fig. 2b (ii)). At the last step (Fig. 2b(iii)), due to high cooling rate, holes were formed on the center of surface and piled up materials at the edge of dimples were created [27]. According to this mechanism, between various laser parameters affecting the microstructure of surface, irradiance properties, as well as laser exposure time, are very crucial [28]. In this study, due to the constant power of the input beam, the effective parameter to control the depth of the molten pool was the beam scan rate, which modulated the residence time of the laser beam on the surface. In this way, reduction in the speed of beam scan from 10 mm/s to 0.5 mm/s enhanced the time of beam placement at a single point leading to a greater depth of dimples from 3 ± 0.3 μm to 6.2 ± 0.3 μm. This result was similarly reported in previous research on 316 L stainless steel revealing that power of irradiance and residence time of CO_2 laser beam affected roughness and depth of melted zone [28]. Kumar [29] studied the role of Nd: YAG laser parameters on the depth and width of the treated zone of Ti6Al4V substrate. They showed that increasing the scan rate from 2.5 to 25 mm/s led to reduce in the treated zone depth from 0.5 to 0.2 mm and the treated width from 1.9 to 1.2 mm.

In addition to the depth and width of micro-dimples, the laser process could simultaneously affect the microstructure of the substrates. Fig. 3 shows the optical and SEM images of the as-received and laser-treated samples consisting of the lowest (L1 sample) and the highest (L4 sample) area fractions of the textured zones. It needs to mention that, α phase appears light color in the optical micrographs and the darker color in the SEM images. According to the optical micrograph and SEM images, as-received Ti6Al4V consisted of fully lamellar microstructure with the grain size of 6–8 μm. This microstructure consisted of the α-Ti matrix and β phase which distributed uniformly in the matrix. After the laser treatment process, the microstructure of the samples and the distribution of α and β phases was changed. However, the distribution of α and β phases was similar at two different treated alloys. According to the optical and SEM images, laser treatment resulted in the formation of higher α content with acicular morphology around the dimples (detected using red arrows). In addition, smaller β phase (darker region) was distributed in the whole

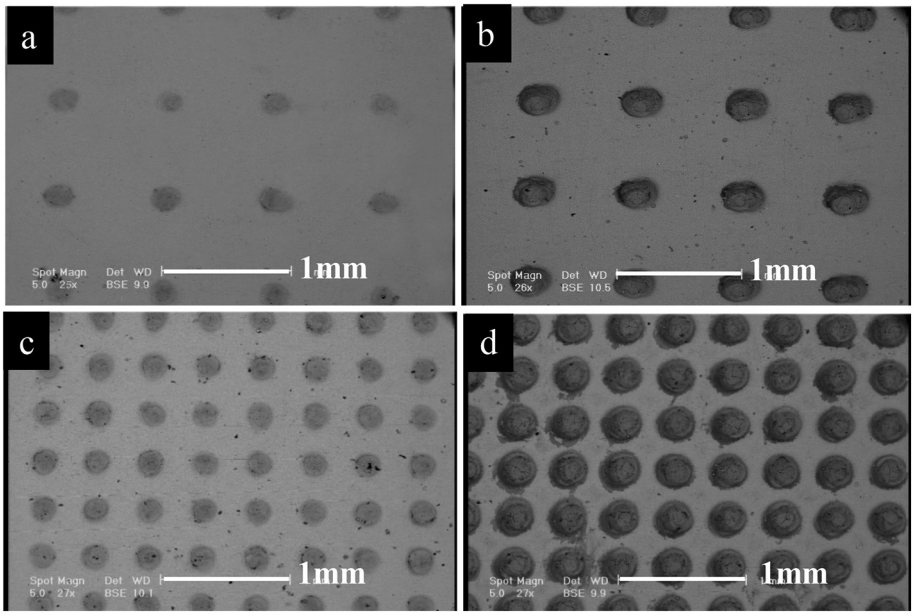

Fig. 1. SEM micrographs of various surface textured samples corresponding to the micro-dimple density: (a) 6.5% (L1 sample), (b) 13.2% (L2 sample), (c) 21.2% (L3 sample) and (d) 42.6% (L4 sample).

microstructure, except around the micro-dimples. It might be due to rapid solidification of the melted zone leading to the transformation of α + β into α-acicular (β-converted) and adsorption of oxygen from the environment. This fine α acicular martensite phase has a hexagonal closed packed structure with high hardness, but a relatively low toughness and flexibility which increases the resistance to wear and corrosion [28]. Depending on the scan rate, the thickness of α-acicular phase was changed. In this respect, L3 sample revealed the largest thickness of α-acicular (20 μm). Furthermore, the gradient of grain size could be detected on the surface of samples. While the grain size of L1 sample at around the melted zone was in the range of 1–3 μm (point 1 in Fig. 3e), it was about 3–8 μm apart from the melted zone (point 2 in Fig. 3e). Moreover, according to optical micrographs, compared to L1, L4 sample consisted of higher α acicular (lighter phase showing with blue elliptic shape) around the dimples. The grain size between two dimples was about 2–4 μm (point 3 in Fig. 3h), which was finer than L1 sample. It could be due to the slower cooling rate of L1 than L3.

The phase transformation could be demonstrated via XRD technique. XRD patterns of the as-received and laser-treated samples (Fig. 4) confirmed that laser process changed the amounts of α and β phases, depending on the beam scan rate. XRD pattern of as-received Ti6Al4V consisted of the majority of α-Ti crystallographic planes ((100), (101), (102), (110), (112), (201) and (104) at $2\theta = 35.4^\circ$, 40.2°, 53.1°, 63.2° and 76.5°, respectively), and β-Ti crystallographic planes ((110) and (211) at $2\theta = 38.4^\circ$ and 70.8°, respectively) [28]. Increasing the number of micro-dimples from L1 to L4 sample led to enhance in the ratio of α phase to β phase and formation of various types of titanium oxides (e.g. anatase, rutile, and Ti_2O_3) during or after laser process. Reduction of β-Ti content in the structure might be related to the stabilization of α acicular martensite through high cooling rate [16]. In addition, the formation of titanium oxides could be due to the reaction between titanium with oxygen during and after laser processing. Formation of titanium oxide was similarly reported in previous researches focusing on the laser surface treatment of Ti6Al4V for biomedical implants and could be advantageous for both improved wear resistance and biocompatibility [12].

The changes in the structural properties of the laser-treated Ti6Al4V could considerably modulate the hardness of samples. The micro-hardness profile of the various samples as a function of distance from one dimple is presented in Fig. 5. Generally, laser-treatment improved the micro-hardness of the as-received alloy from the substrate to the edge of dimples, depending on the laser texture type. Noticeably, at L3 sample, while maximum hardness was estimated about 635 ± 21 Hv at the edge of micro-dimples, it was reduced to about 347 ± 16 Hv at the distance between two dimples, at L2 sample. Enhanced micro-hardness in the melted zone might be related to the uniformity of the microstructure, reduced β phase and formation of acicular α (martensite) with hcp structure which formed through rapid quenching after laser process. Acicular α with high hardness and low ductility and toughness led to enhanced micro-hardness of Ti6Al4V with the higher density of micro-textured samples (L3 sample). In addition, the improvement in the hardness of textured Ti6Al4V might be due to formation of oxide phases in textured zone (such as anatase, rutile and Ti_2O_3). Similarly, Singh et al. [30] reported the improvement in the hardness of the laser treated Ti6Al4V alloys by Nd: YAG laser owing to the formation of oxide phases in texture zone. Furthermore, enhanced micro-hardness on the laser surface treated samples might be attributed to the reduction of grain size according to Hall-Petch relation [31].

The wettability is one of the crucial features of surface engineering for biomedical materials. According to Table 1, it could be concluded that surface texturing remarkably promoted the surface wettability of samples. Noticeably, the water contact angle significantly reduced from 49 ± 4° (at as-received Ti6Al4V) to 33 ± 5° (at L3 sample). However, it could be concluded that various mechanisms simultaneously affected the water contact angle consisting of surface roughness and chemical composition, based on Wenzel and Cassie-Baxter models and their combination [32]. Results showed that micro-dimple formation with the lowest density (L1 sample) considerably enhanced the hydrophilicity of the Ti6Al4V due to superior roughness and formation of oxide layer on the surfaces. However, increasing the dimple area ratio to 13.2% (L2 sample) enhanced water contact angle compared to L1 sample. It might be due to the pile-up phenomenon around the dimples (Fig. 2) limiting the contact surface of the droplet and substrate to the bumps leading to enhanced water contact angle. Compared to L2 sample, water contact angle on the L3 sample significantly reduced owing to the formation of surface oxides with higher hydrophilicity and less pile up. This result was similarly reported in the TiO_2–containing layer formed on the laser treated samples [33]. Finally, the enhanced density of dimples at L4 sample (42.6%) resulted in reduced hydrophilicity of samples compared to L3 samples. It could be due to the pile

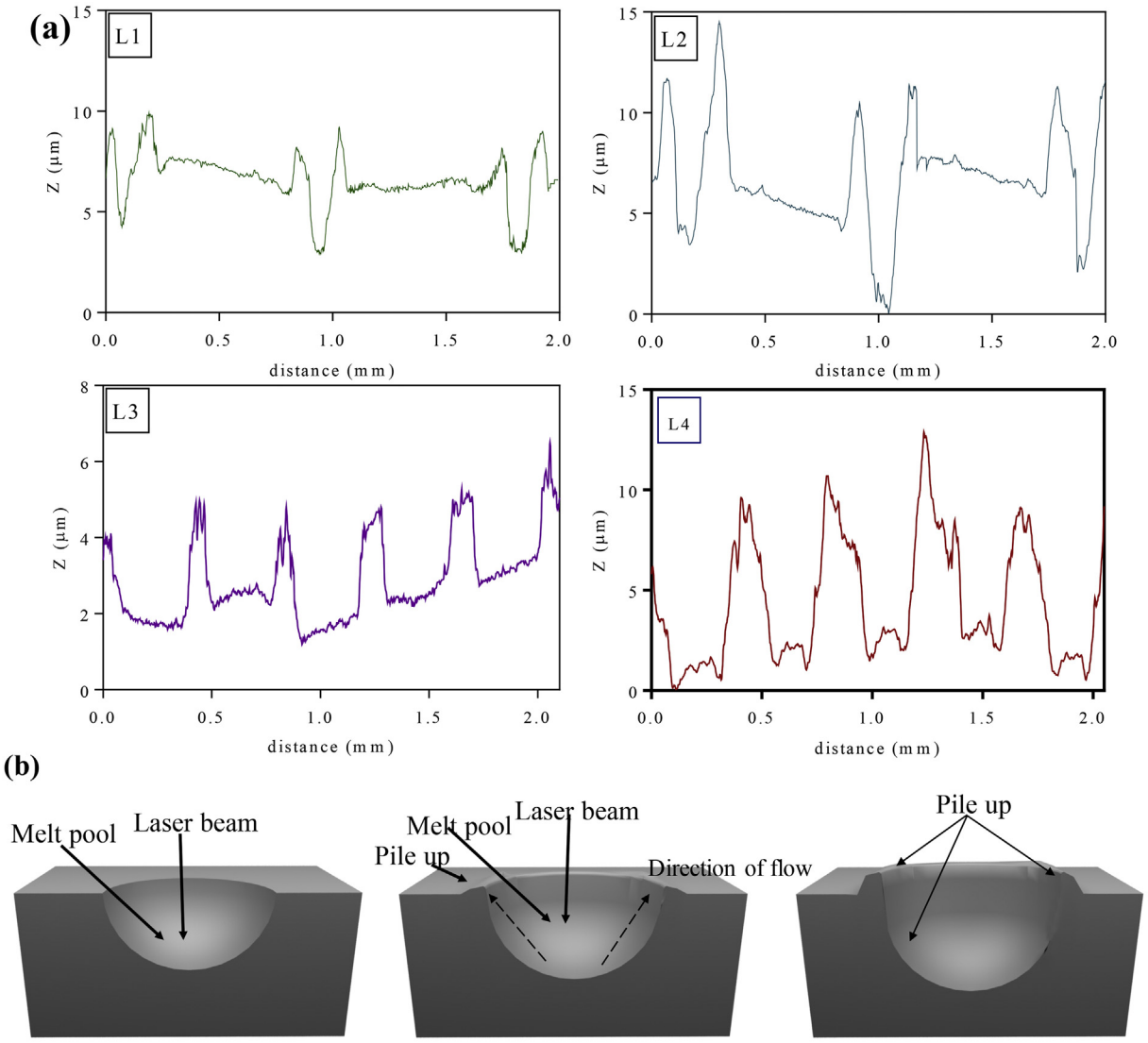

Fig. 2. (a) The changes of micro-dimple depth in various samples obtained via surface roughness tester. (b) The schematic showing the formation of micro-dimples during laser process.

up phenomenon around the dimples. Our results confirmed that the wettability of the surfaces depended on the laser process parameters which directly affected by chemical composition, topography, and roughness, as similarly reported in previous researches [33]. According to Wenzel's equation, enhanced surface roughness resulted in reduced water contact angle and consequently enhanced the hydrophilicity of samples [34]. In addition to surface roughness, surface oxidization could noticeably result in improved surface wettability [34]. According to XRD patterns, laser process resulted in the formation of various titanium oxide types consisting of TiO, TiO_2 (rutile and anatase) and Ti_2O_3. In addition, laser texturing via surface melting process could meaningfully improve the surface energy of samples followed by the wettability of surfaces [23].

3.2. Biological properties of laser-textured Ti6Al4V alloy

According to previous researches, cell responses were affected by surface properties including chemical composition and surface roughness [35]. In order to evaluate the role of various laser-treated surfaces on the cell responses, MG63 cells were cultured on the samples and cell morphology and proliferation were evaluated. From MTT results (Fig. 6), it could be found that, after 3 days of culture, the cell proliferation was significantly higher than that of on the control. Furthermore, our results confirmed that laser texturing significantly changed cell proliferation, depending on the laser process condition. For instance, while the cell survival after 3 days of culture on Ti6Al4V sample was 112 ± 37 (%control), it was meaningfully improved (206 ± 7 (%control)) at L4 sample thanks to considerably endorsed hydrophilicity. In contrary, the proliferation of cells on the L2 was 1.6 times less than that of on the untreated Ti6Al4V.

SEM images of MG63 cells cultured on the samples for 3 days are presented in Fig. 7a. Results showed that the cells spread on the surface of all samples, specifically the micro-textured samples. While the cells were not expanded well on the surface of Ti6Al4V, they covered the micro-dimples of textured samples. Similarity, Mirhosseini et al. [23] similarly reported that despite the biocompatibility of Ti, cell growth on the surface of untreated Ti was not uniform in whole surface. Cells were gathered in some areas. However, our results discovered that the fraction of laser-treated samples coved by cells was different, depending on the laser process condition. The area fraction of substrates covered by cells is presented in Fig. 7b. Between various laser-treated samples, more fraction area of L1 (78 ± 2%), L3 (72 ± 6%) and L4 (82 ± 9%) samples were covered by cells. Moreover, no detectable cells were found on the micro-dimples of L2 sample, and only a few numbers of

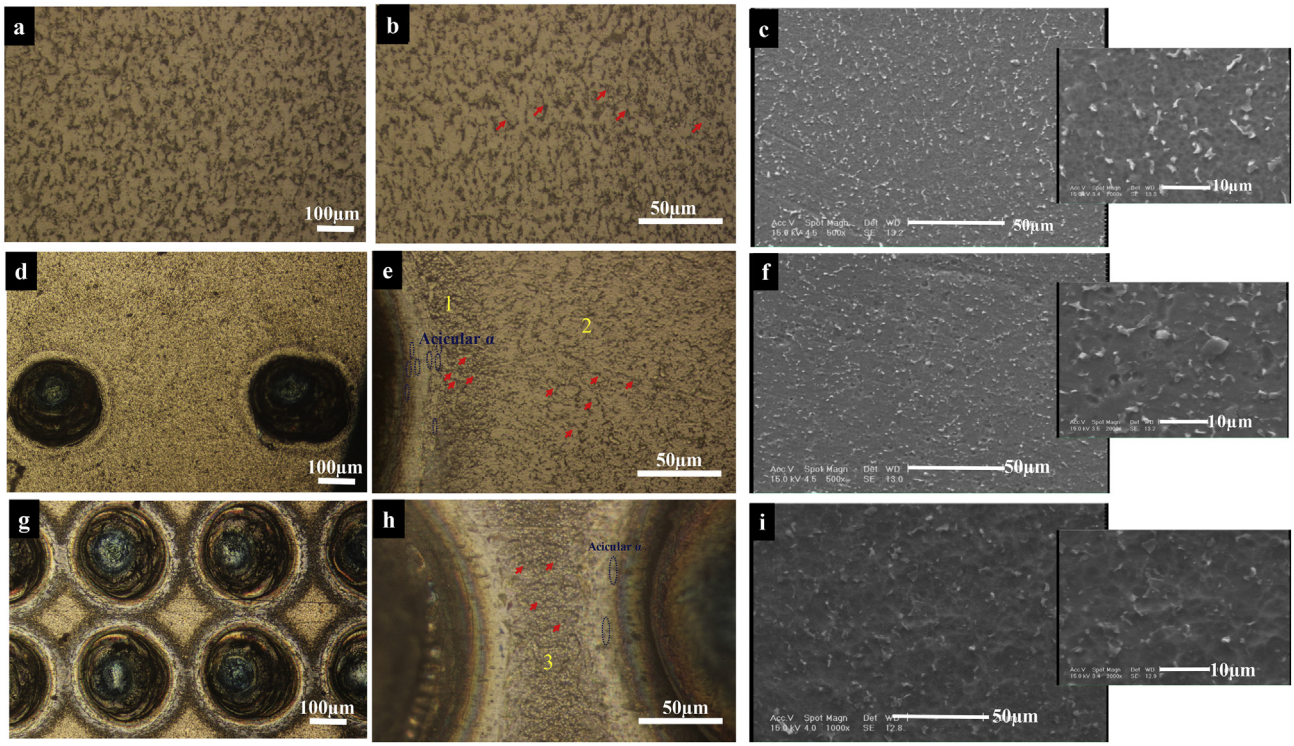

Fig. 3. Optical and SEM images of various Ti6Al4V based samples at different magnifications: (a (100×), b (500×) and c) untreated Ti6Al4V, (d (100×), e (500×) and f) L1 sample, (g (100×), h (500×) and i) L4 sample.

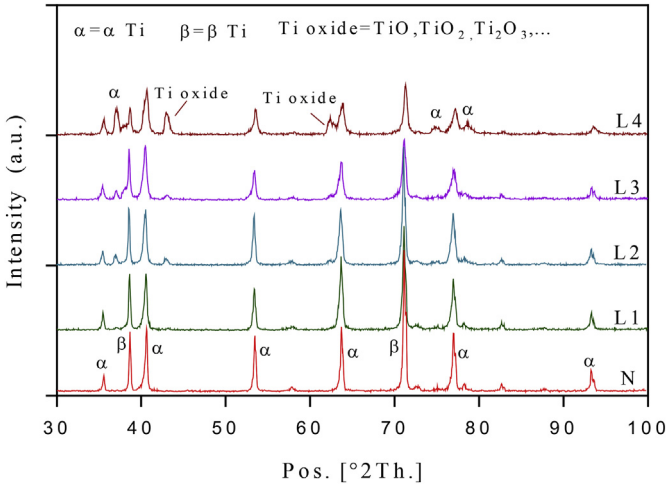

Fig. 4. X-ray diffraction patterns of untreated (N) and various surface-treated samples.

cells could be detected between the dimples. These results might be due to the pile-up around the micro-dimples on L2 sample leading to reduced hydrophilicity of this sample compared to others. Similarly, Georgi et al. [36] showed that the proliferation of fibroblasts enhanced with increasing surface wettability. Chen et al. [18] investigated initial attachment and orientation of osteoblast-like cells on longitudinally- and transversally-oriented micro-grooves developed using the laser irradiation on Ti6Al4V surfaces. They showed that cell attachment and spreading was significantly improved on longitudinally- and transversally-oriented micro-grooves and enhanced with increasing culture time. Generally, substrate characteristics, such as surface energy, chemistry, roughness, and topography are of crucial factors for the adsorption of proteins and consequently cell attachment and proliferation [37]. Among them, metal oxides formed on metal surfaces are important factors affecting the biological behavior of a substance. Other researches also similarly reported that an increase in surface roughness and surface energy led to improved cell adhesion and proliferation [23].

3.3. Wear characterization of laser-textured samples

One of the crucial issue of Ti6Al4V for biomedical implants, specifically hip and knee prostheses, is its weak wear characteristic. Many parameters are effective on wear behavior of a tribo-system, consisting of contact pressure, sliding distance, velocity, temperature and humidity as well as material characteristics [28,38]. According to mathematical models, metals with lower shear strength have higher friction than metals with high shear strength [28]. Hence, to enhance the surface strength and reduce the friction coefficient and the adhesion wear, surface treatment of Ti-based alloys was recommended [39]. In this study, the role of laser texturing and its parameters on the wear behavior of Ti6Al4V was evaluated. Wear test was performed under the pin-on-disc tribo-system using Ti6Al4V discs with diameter of 50 ± 0.02 mm and a zirconia ball with 10 mm in the diameter and hardness of 1340 Hv, at constant temperature and humidity under a constant speed of 0.1 m/s. In order to assess the wear behavior, the weight loss and friction coefficient of various samples were studied. Primarily, the load test was performed by means of 5, 10, 15, 20 and 25 N loads at a distance of 50 m for each load. The weight loss of the discs at the end of 50 m for each applied load is presented in Supplementary Fig. S2. According to the weight loss result as well as the range of force on the knee joint, 7 N was selected as the appropriate load for next experiments.

To determine the wear mechanisms in each sample, wear test was performed under the load of 7 N and velocity of 0.1 m/s at a distance of 200 m for all samples (Fig. 8). Our results revealed that the weight loss of all textured Ti6Al4V samples (Fig. 8a) was less than that of the as-received Ti6Al4V sample. Noticeably, while the weight loss of as-received Ti6Al4V sample was 2.7 ± 0.1 mg, it was reduced to

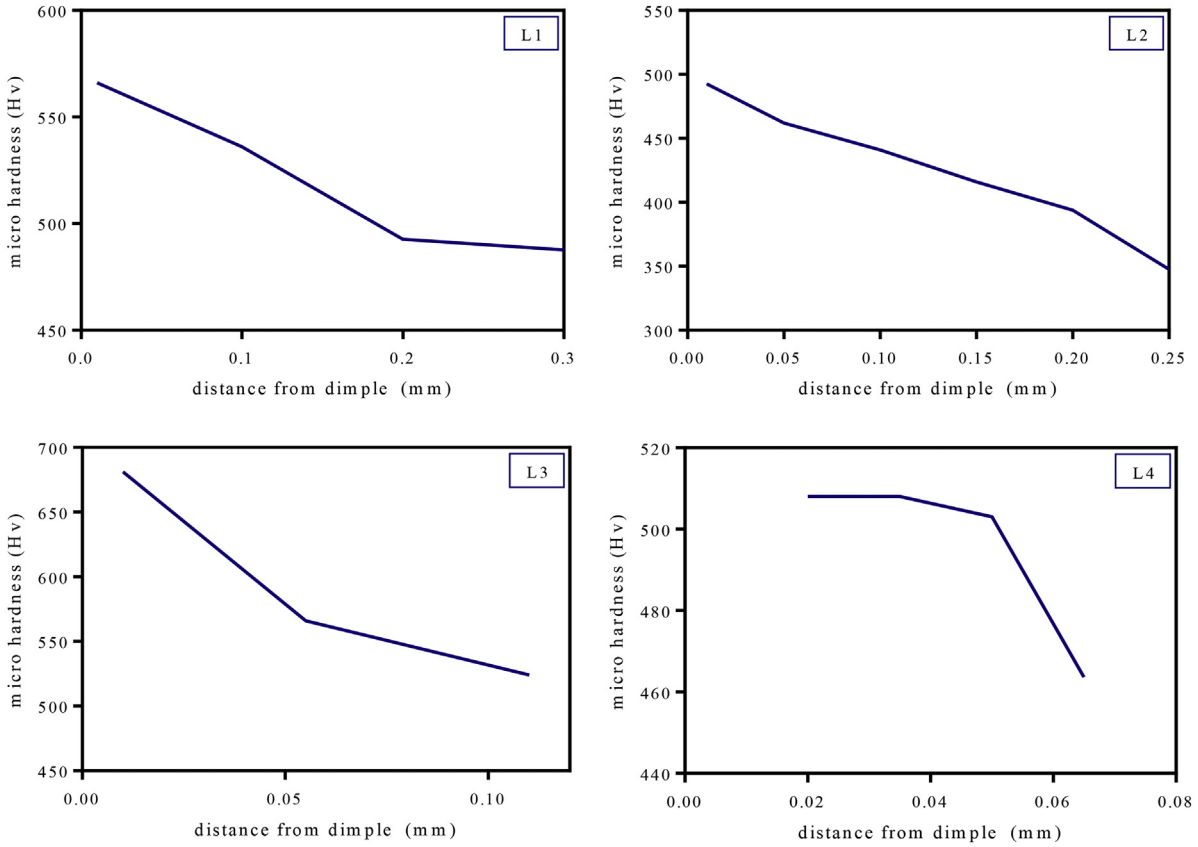

Fig. 5. Micro-hardness profile of various surface-treated Ti6Al4V samples in the distance between micro-dimples, in the load of 100 N.

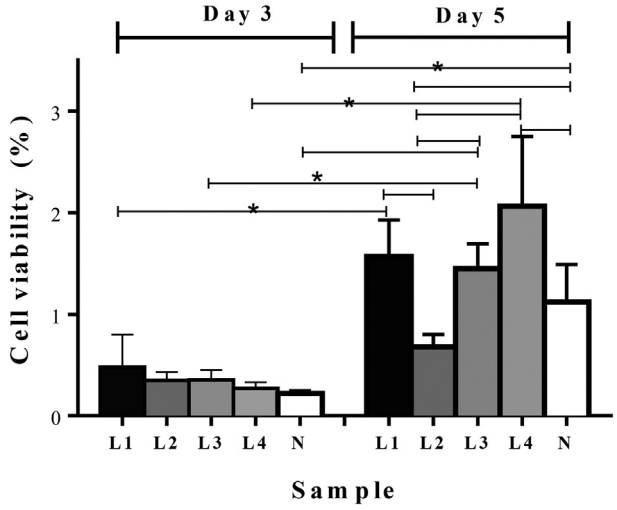

Fig. 6. MTT assays of MG63 cells seeded on untreated (N) and micro-textured Ti6Al4V after 5 days of culture (*: $P < 0.05$).

2.0 ± 0.1 mg at L1 sample, after 200 m of wear test. It is well known that there is always a thin oxide film on the Ti-based alloy surfaces. However, thanks to the weak protection of thin film, this oxide film on the untreated surface could not play a potent role for the surface. At the high loading conditions, in contact with another metal surface, the oxide film was easily removed from the substrate surface, leading to direct contact between the metal and hence severe adhesive wear. The reduction of weight loss in the laser-treated samples compared to as-received one could be attributed to the absorption of wear particles inside the micro-dimples, the hardening of the samples and the formation of surface oxides. Moreover, the existence of micro-dimples acted as a pool for wear particles to trap them. In addition, the depth, diameter and shape of dimples were effective on the amount of wear debris which trapped inside pools. For instance, the weight loss of micro-textured Ti6Al4V enhanced from L1 sample (2 ± 0.05 mg) to L4 sample (2.7 ± 0.05 mg). It might be due to less hardness of L4 samples which resulted in enhanced weight loss compared to other micro-textured samples. Moreover, the pile-up materials at the edge of the dimples at L2 and L4 samples due to the less scan speed could control the weight loss during the wear test. The pile-up materials at the edge of dimples could enhance surface roughness and counterfaces leading to the increased wear rate and vibration at the contact surface between the pin and the disc [40].

The friction coefficient of samples under a load of 7 N and a distance of 200 m was also investigated. According to Fig. 8b and Supplementary Fig. S3, it could be found that the friction coefficient significantly reduced from 0.43 ± 0.05 (at as-received Ti6Al4V) to 0.31 ± 0.06 (at L3 sample). It might be related to the improved surface hardness of the micro-textured surfaces, the function of these dimples to reserve wear particles, and formation of the oxide layer in the laser process. As mentioned, these cavities acted like sinks in which the wear particles accumulated there, and prevented from the wear of the three-body scratches which could be occurred due to the free movement of wear particles between the ball and disc interfaces. However, increasing the dimple area ratio to 42.5% (at L4 sample) resulted in enhanced friction coefficient. Since the distances between the cavities in the L4 sample (120 μm) was less than that of other samples (600, 520 and 220 μm for L1, L2, and L3, respectively), it could reduce the contact surface which resulted in the concentration of stress at the contact point leading to the enhanced destruction and wear on the surface. Similarly, Kumaria et al. [20] examined the friction coefficient of Ti6Al4V samples which were textured using ArF excimer laser. They found that friction coefficient of Ti6Al4V reduced from 1 to < 0.55. Moreover, Hu et al. [21] investigated the friction coefficient of Ti6Al4V against steel pins at

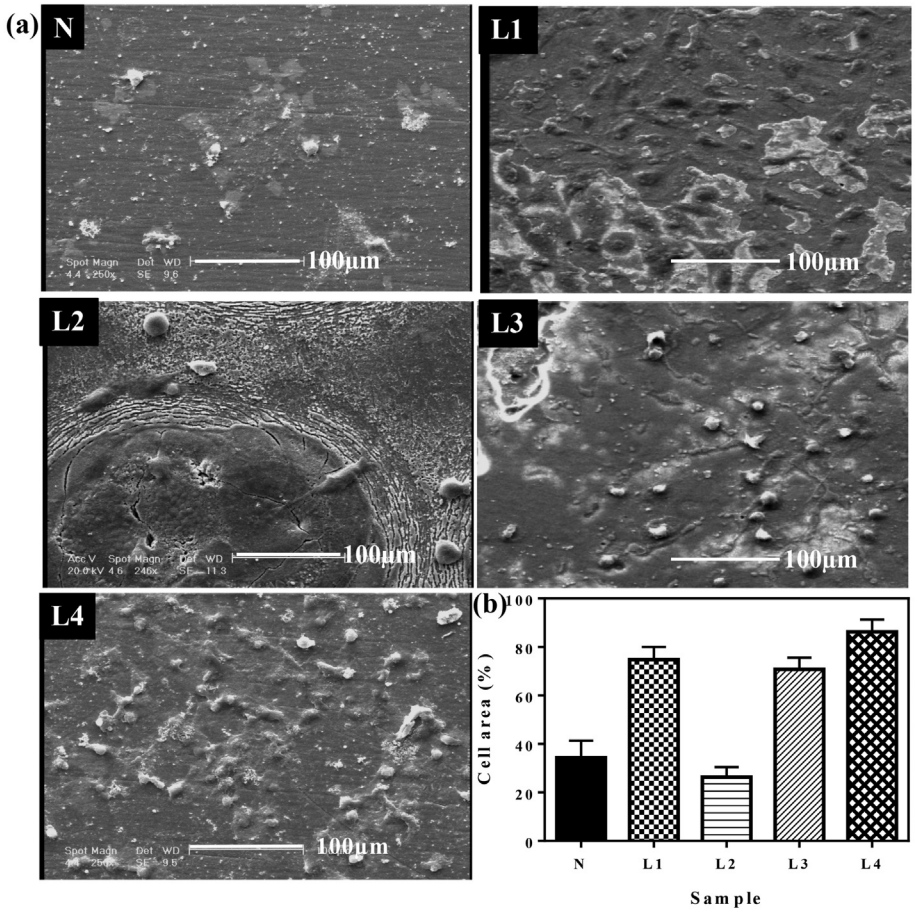

Fig. 7. MG63 cell morphology on the various Ti6Al4V samples: (a) SEM images of MG63 cells cultured on various Ti6Al4V samples. (b) Cell spreading, the fraction of the area of surface samples covered with MG63 cells.

different dimple densities (13%, 23%, and 44%). They revealed that under low applied load (1 N), due to the aggregation of debris inside dimples, the friction coefficient decreased from 0.8 in the un-textured sample to about 0.2 in the high dimpled-density sample. Nevertheless, when the applied load increased to 10 N, the effective area of contact enhanced leading to the increased friction coefficient. Our results confirmed that between various samples consisting of various dimple densities, sample L3 revealed the optimized condition to control friction coefficient making it ideal for load-bearing applications.

3.4. Analysis of worn surfaces

The worn surfaces of the un-textured and laser-textured samples are presented in Fig. 9. The presence of rough grooves and a deep appearance at the surface of un-textured Ti6Al4V confirmed the presence of abrasive wear mechanism. Moreover, the plastic shape changes could be detected at the worn surface of un-textured Ti6Al4V due to the low shear strength of the Ti6Al4V alloy leading to adhesion and smearing the wear particles on the surface. This mechanism was attributed to the separation of particles from the surface and their accumulation at the edge of the grooves. This mechanism was similarly reported in previous

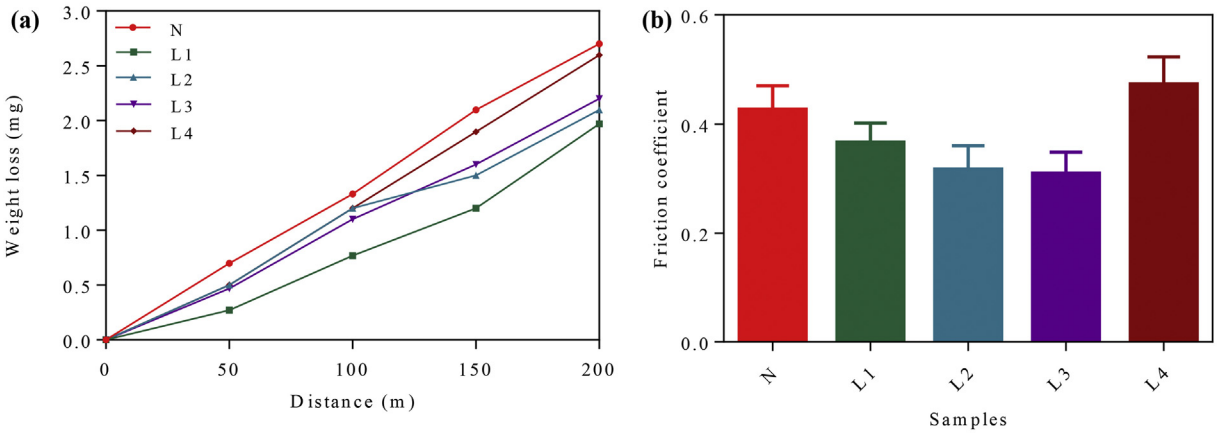

Fig. 8. (a) The weight loss of samples as a function of the sliding distance under 7 N loading. (b) Friction coefficient graph of untreated (N) and laser-treated samples.

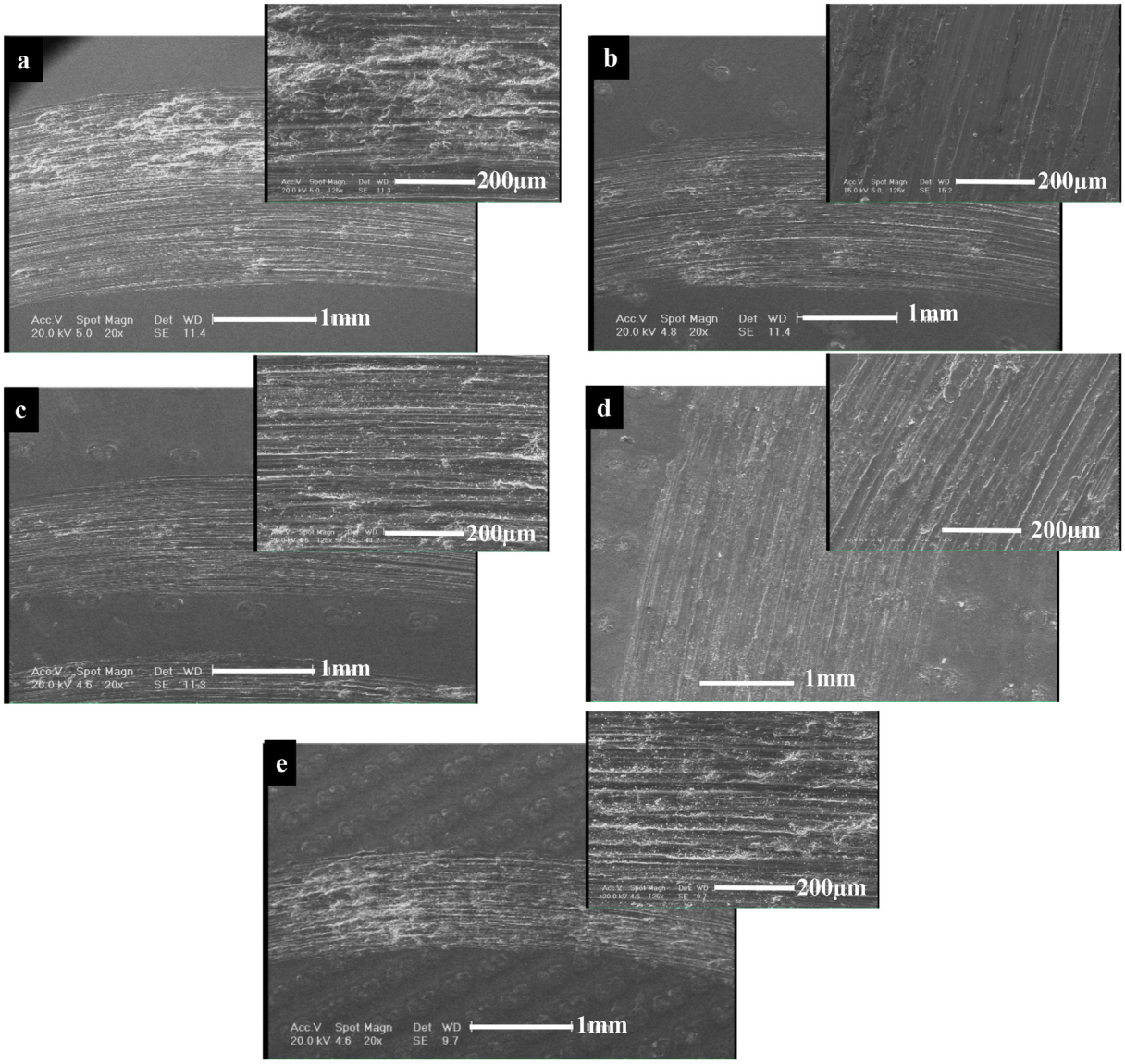

Fig. 9. SEM micrographs of worn surfaces of the samples under dry friction at 7 N and distance of 200 m: (a) untreated Ti6Al4V (N), (b) L1, (c) L2, (d) L3, (e) L4.

researches [31]. Compared to the untreated sample, the grooves formed on the L1 sample were softened, and the amount of lamination and plastic shape changes were far less than untreated alloy. It might be due to the trapping of the wear particles inside the dimples and the reduction of stress concentration at the point of contact between the ball and the disc. At L2 and L3 samples, there was less spoilage, and the wear mechanism was more abrasive with parallel grooves. Moreover, some micro-cracks were identified, due to the fatigue wear mechanism. Finally, the surface of sample L4 consisted of a large variety of plastic deformation and cracks while deep grooves were detected. The cross-section image of the worn surface could help to indicate the wear mechanisms. The cross-section images of un-textured Ti6Al4V, L1 and L3 samples after the wear test are presented in Fig. 10a. While the blunder could be detected at un-textured Ti6Al4V clearly, L1 sample consisted of parallel and pitting grooves at the edges of grooves. Furthermore, worn surface of sample L3 consisted of a very little blunder at the edges of dimples. These results demonstrated that increasing the density of the dimples from 6.5% in L1 to 21.2% in L3 sample resulted in the formation of parallel grooves on the surface indicating abrasive wear was reduced. It might be due to the trapping of wear particles inside the dimples and the reduction of three-body abrasive wear. The similar mechanism was reported in previous researches. For instance, Singh et al. [31] reported plastic deformation and adhesion mechanism for laser treated Ti6Al4V. In another study, Chikarakara [28] investigated the effects of high-speed laser surface modification to form channel-like grooves on Ti6Al4V for biomedical implants by using the CO_2 laser. They showed the transformation in microstructure and increasing in micro-hardness of surface and wear resistance of the alloy. The similar wear mechanism was reported in this study.

In order to evaluate the mechanism of wear in various samples, SEM images of wear debris were investigated (Fig. 10b). Results showed the formation of wear particles with various morphologies, depending on the laser-texturing process of the Ti6Al4V alloy. According to previous researches, while the smaller debris was the product of the abrasive and/or adhesive wear mechanism, larger sheet–like particles was related to the delamination and fatigue wear [41]. Our results revealed that the worn surface of the un-textured Ti6Al4V sample consisted of the wear particles with both plate and sheet-shaped morphologies confirming the abrasive mechanism (plate-shaped particles) as well as delamination mechanism due to fatigue wear (sheet-shaped particles). However, according to SEM images, delamination and fatigue wear were the main mechanisms. In contrary to the un-textured Ti6Al4V sample, the plate-shaped of wear particles obtained from L1 sample showed the abrasive mechanism as the main mechanism. Furthermore,

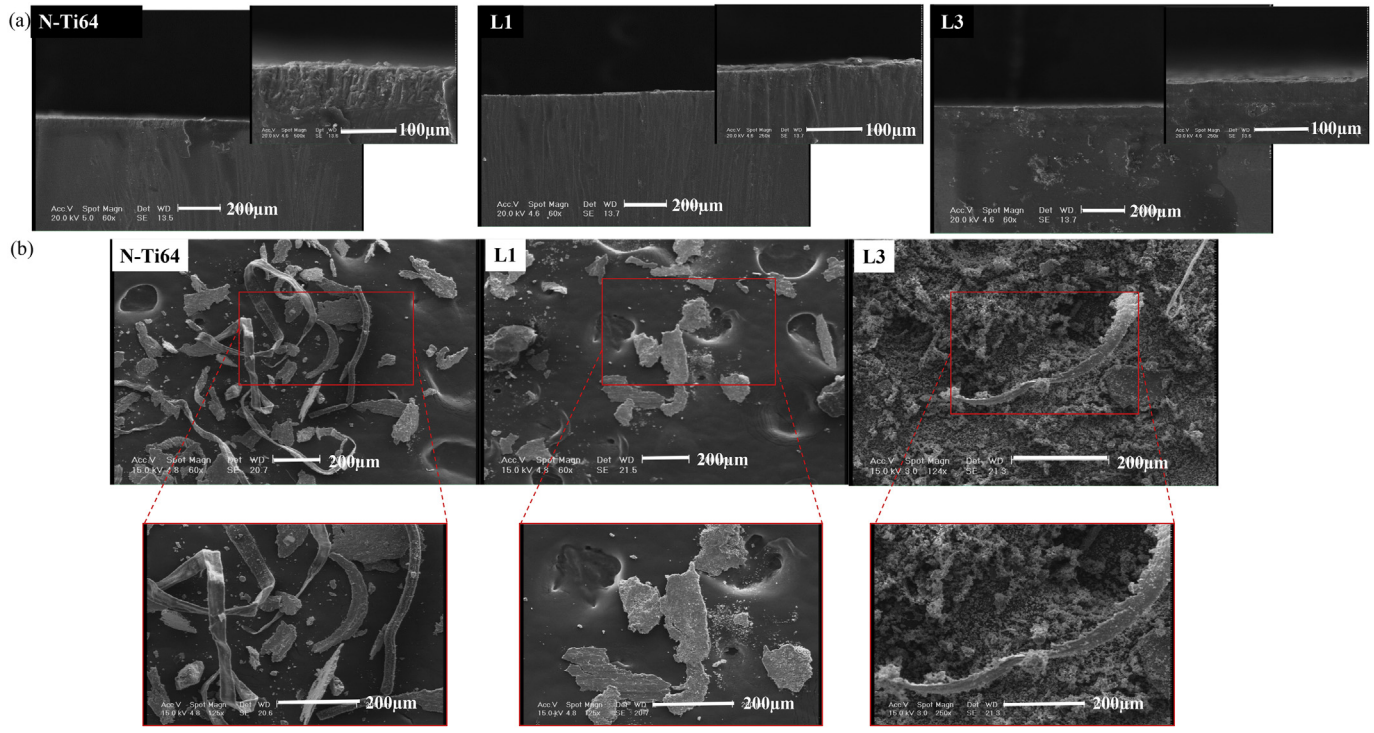

Fig. 10. (a) Cross-section images of the worn surface under the load of 7 N and distance of 200 m for untreated Ti6Al4V (N), L1 and L2 samples. (b) SEM micrographs of wear particles of untreated Ti6Al4V (N), L1 and L3 samples.

L3 sample consisted of finer plate debris revealing the abrasive wear as the main mechanism. This behavior might be due to the significantly higher hardness of L3 sample (680 ± 21 Hv) compared to L1 and untextured Ti6Al4V.

Our results confirmed that the modulation of several characteristics, such as surface hardness and hydrophilicity, could noticeably affect the biological and tribological responses of the Ti6Al4V alloy. According to the features of micro-dimpled samples with various geometries, L3 sample revealed the optimized biological and tribological responses making it ideal for knee implant materials.

4. Conclusion

In this study, laser texturing of Ti6Al4V alloy with four different dimple geometries were developed using CO_2 laser with different beam scan rates (0.5 mm/s (L4 sample), 1 mm/s (L1 sample), 5 mm/s (L3 sample) and 10 mm/s (L1 sample)). From the comprehensive research, the following conclusions are presented:

(1) Laser texturing of Ti6Al4V were successfully developed using CO_2 laser leading to the formation of periodic micro-dimple arrays with various geometries, depending on the scan rate of the beam (0.5–10 m/s)
(2) Improvement of micro-hardness and wettability was accomplished due to modulation of microstructure and chemical composition of micro-patterned Ti6Al4V, depending on the scan rate of the laser beam.
(3) MG63 cell attachment, proliferation and spreading were effectively promoted using laser-texturing process, depending on the surface geometry. Noticeably, after 3 days of culture, the cell proliferation on the L3 sample was 1.5 and 2.3 times higher than that of on the Ti6Al4V and L2 samples, respectively.
(4) The area fraction of samples covered with MG63 cells was significantly enhanced on L1, L3 and L4 samples compared to control (Ti6Al4V).
(5) Laser texturing resulted in significantly improvement of wear resistance via reduced weight loss and the friction coefficient of samples. It could be attributed to the promoted micro-hardness, controlled microstructure and formation of oxide phase on the surface.

Appendix A. Supplementary data

Supplementary data to this article can be found online at https://doi.org/10.1016/j.surfcoat.2019.01.113.

References

[1] M.B. Nasab, M.R. Hassan, B.B. Sahari, Metallic biomaterials of knee and hip—a review, Trends Biomater. Artif. Organs 24 (2010) 69–82.
[2] K.J. Bozic, S.M. Kurtz, E. Lau, K. Ong, V. Chiu, T.P. Vail, H.E. Rubash, D.J. Berry, The epidemiology of revision total knee arthroplasty in the United States, Clin. Orthop. Relat. Res. 468 (2010) 45–51.
[3] M. Niinomi, Mechanical properties of biomedical titanium alloys, Mater. Sci. Eng. A 243 (1998) 231–236.
[4] N. Poondla, T.S. Srivatsan, A. Patnaik, M. Petraroli, A study of the microstructure and hardness of two titanium alloys: commercially pure and Ti–6Al–4V, J. Alloys Compd. 486 (2009) 162–167.
[5] H. Dong, T. Bell, Enhanced wear resistance of titanium surfaces by a new thermal oxidation treatment, Wear 238 (2000) 131–137.
[6] A. Molinari, G. Straffelini, B. Tesi, T. Bacci, Dry sliding wear mechanisms of the Ti6Al4V alloy, Wear 208 (1997) 105–112.
[7] K. Holmberg, A. Matthews, Coating Tribology: Properties, Techniques, and Applications in Surface Engineering, Elsevier, 1994.
[8] T. Hanawa, S. Hiromoto, A. Yamamoto, N. Maruyama, K. Nakazawa, Metallic biomaterials in body fluid and their surface modification, Structural Biomaterials for 21th Century, 2001, pp. 145–156.
[9] C. Peterson, B. Hillberry, D. Heck, Component wear of total knee prostheses using Ti-6Al-4V, titanium nitride coated Ti-6Al-4V, and cobalt-chromium-molybdenum femoral components, J. Biomed. Mater. Res. A 22 (1988) 887–903.
[10] H. Dong, A. Bloyce, P. Morton, T. Bell, Surface engineering to improve tribological performance of Ti–6Al–4V, Surf. Eng. 13 (1997) 402–406.
[11] D.G. Bansal, O.L. Eryilmaz, P.J. Blau, Surface engineering to improve the durability and lubricity of Ti–6Al–4V alloy, Wear 271 (2011) 2006–2015.
[12] W. Pfleging, R. Kumari, H. Besser, T. Scharnweber, J.D. Majumdar, Laser surface textured titanium alloy (Ti–6Al–4V): part 1–surface characterization, Appl. Surf. Sci. 355 (2015) 104–111.
[13] A. Bagno, C. Di Bello, Surface treatments and roughness properties of ti-based biomaterials, J. Mater. Sci. Mater. Med. 15 (2004) 935–949.

[14] F. Grizon, E. Aguado, G. Hure, M. Baslé, D. Chappard, Enhanced bone integration of implants with increased surface roughness: a long term study in the sheep, J. Dent. 30 (2002) 195–203.
[15] A. Kurella, N.B. Dahotre, Surface modification for bioimplants: the role of laser surface engineering, J. Biomater. Appl. 20 (2005) 5–50.
[16] A. Biswas, L. Li, T. Maity, U. Chatterjee, B. Mordike, I. Manna, J.D. Majumdar, Laser surface treatment of Ti-6Al-4V for bio-implant application, Lasers Eng. 17 (2007) 59–73.
[17] I. Etsion, State of the art in laser surface texturing, Trans. ASME F J. Tribol. 127 (2005) 248.
[18] J. Chen, J. Ulerich, E. Abelev, A. Fasasi, C. Arnold, W. Soboyejo, An investigation of the initial attachment and orientation of osteoblast-like cells on laser grooved Ti-6Al-4V surfaces, Mater. Sci. Eng. C 29 (2009) 1442–1452.
[19] H. Yu, H. Deng, W. Huang, X. Wang, The effect of dimple shapes on friction of parallel surfaces, Proc. Inst. Mech. Eng. Part J: J. Eng. Tribol. 225 (2011) 693–703.
[20] R. Kumari, T. Scharnweber, W. Pfleging, H. Besser, J.D. Majumdar, Laser surface textured titanium alloy (Ti–6Al–4V)–part II–studies on bio-compatibility, Appl. Surf. Sci. 357 (2015) 750–758.
[21] T. Hu, L. Hu, Q. Ding, Effective solution for the tribological problems of Ti-6Al-4V: combination of laser surface texturing and solid lubricant film, Surf. Coat. Technol. 206 (2012) 5060–5066.
[22] Y. Qin, D. Xiong, J. Li, Tribological properties of laser surface textured and plasma electrolytic oxidation duplex-treated Ti6Al4V alloy deposited with MoS2 film, Surf. Coat. Technol. 269 (2015) 266–272.
[23] N. Mirhosseini, P. Crouse, M. Schmidth, L. Li, D. Garrod, Laser surface micro-texturing of Ti–6Al–4V substrates for improved cell integration, Appl. Surf. Sci. 253 (2007) 7738–7743.
[24] A. Amanov, R. Tsuboi, H. Oe, S. Sasaki, The influence of bulges produced by laser surface texturing on the sliding friction and wear behavior, Tribol. Int. 60 (2013) 216–223.
[25] L. Duisabeau, P. Combrade, B. Forest, Environmental effect on fretting of metallic materials for orthopaedic implants, Wear 256 (2004) 805–816.
[26] N. Golafshan, M. Kharaziha, M. Fathi, Tough and conductive hybrid graphene-PVA: alginate fibrous scaffolds for engineering neural construct, Carbon 111 (2017) 752–763.
[27] N.B. Dahotre, S.R. Paital, A.N. Samant, C. Daniel, Wetting behaviour of laser synthetic surface microtextures on Ti–6Al–4V for bioapplication, Philos. Trans. R. Soc. Lond. A: Math. Phys. Eng. Sci. 368 (2010) 1863–1889.
[28] E. Chikarakara, Laser Surface Modification of Biomedical Alloys, Dublin City University, 2012.
[29] V. Kumar, Process parameters influencing melt profile and hardness of pulsed laser treated Ti–6Al–4V, Surf. Coat. Technol. 201 (2006) 3174–3180.
[30] R. Singh, S. Tiwari, S.K. Mishra, N.B. Dahotre, Electrochemical and mechanical behavior of laser processed Ti–6Al–4V surface in ringer's physiological solution, J. Mater. Sci. Mater. Med. 22 (2011) 1787.
[31] R. Singh, A. Kurella, N.B. Dahotre, Laser surface modification of Ti—6Al—4V: wear and corrosion characterization in simulated biofluid, J. Biomater. Appl. 21 (2006) 49–73.
[32] A. Cunha, Multiscale Femtosecond Laser Surface Texturing of Titanium and Titanium Alloys for Dental and Orthopaedic Implants, Université de Bordeaux, 2015.
[33] A. Cunha, A.P. Serro, V. Oliveira, A. Almeida, R. Vilar, M.-C. Durrieu, Wetting behaviour of femtosecond laser textured Ti–6Al–4V surfaces, Appl. Surf. Sci. 265 (2013) 688–696.
[34] L. Hao, J. Lawrence, Wettability modification and the subsequent manipulation of protein adsorption on a Ti6Al4V alloy by means of CO_2 laser surface treatment, J. Mater. Sci. Mater. Med. 18 (2007) 807–817.
[35] B.D. Boyan, T.W. Hummert, D.D. Dean, Z. Schwartz, Role of material surfaces in regulating bone and cartilage cell response, Biomaterials 17 (1996) 137–146.
[36] G. Altankov, F. Grinnell, T. Groth, Studies on the biocompatibility of materials: fibroblast reorganization of substratum-bound fibronectin on surfaces varying in wettability, J. Biomed. Mater. Res. A 30 (1996) 385–391.
[37] T. Lee, E. Chang, C.-Y. Yang, Attachment and proliferation of neonatal rat calvarial osteoblasts on Ti6Al4V: effect of surface chemistries of the alloy, Biomaterials 25 (2004) 23–32.
[38] G. Straffelini, A. Molinari, Dry sliding wear of Ti–6Al–4V alloy as influenced by the counterface and sliding conditions, Wear 236 (1999) 328–338.
[39] T. Baker, Laser surface modification of titanium alloys, Surface Engineering of Light Alloys, Elsevier, 2010, pp. 398–443.
[40] M. Mosleh, N.P. Suh, Wear particles of polyethylene in biological systems, Tribol. Trans. 39 (1996) 843–848.
[41] M. Mosleh, P.J. Blau, D. Dumitrescu, Characteristics and morphology of wear particles from laboratory testing of disk brake materials, Wear 256 (2004) 1128–1134.